Enantiomer-specific state transfer of chiral molecules in cyclic three-level systems with SU(2) structures

Jian-Jian Cheng,[1] Yu-Yuan Chen,[2] Yong Li,[3,4,*] and Lin Zhang[5,†]

[1]*Beijing Computational Science Research Center, Beijing 100193, China*
[2]*School of Integrated Circuits, Tsinghua University, Beijing 100084, China*
[3]*Center for Theoretical Physics and School of Science, Hainan University, Haikou 570228, China*
[4]*Synergetic Innovation Center for Quantum Effects and Applications, Hunan Normal University, Changsha 410081, China*
[5]*School of Physics and Information Technology, Shaanxi Normal University, Xi'an 710119, China*

(Received 30 September 2022; accepted 10 January 2023; published 23 January 2023)

We propose a streamlined method of fast enantiomer-specific state transfer (ESST) of chiral molecules in cyclic three-level systems. Such three-level enantiomers are chirality-dependent systems driven by one of the three Rabi frequencies differing with a sign for the left- and right-handed chiral molecules. When the Hamiltonian of the three-level chiral molecules possesses the specific SU(2) algebraic structure, the populations transferred to the two excited states are shown to be exchanged between the left- and right-handed chiral molecules if they are initially prepared in their ground states. By employing unitary SU(2) transformation and inversely engineering time-dependent Hamiltonians with designed Rabi frequencies, we can make the left- and right-handed chiral molecules evolve respectively to different excited states from their initial ground states simultaneously. Thus a fast ESST is achieved.

DOI: 10.1103/PhysRevA.107.013718

I. INTRODUCTION

A molecule is chiral when it cannot be superposed on its mirror image via translations and rotations. Chiral molecules contain two types, e.g., left- and right-handed chiral molecules [1] (often called enantiomers). They play important roles in contemporary science, such as chemistry [2], biotechnologies [3], and pharmaceutics [4]. Enantiodiscrimination [5] (as well as enantioseparation [6,7] and enantioconversion [8]) of chiral molecules is a significant and difficult challenge in the studies of chiral molecules. The traditional methods of enantiodiscrimination include circular dichroism [9], vibrational circular dichroism [10], optical rotation [11], and Raman optical activity [12], where the interference between magnetic-dipole (or electrical-quadrupole) and electronic-dipole interactions is used. The principle is to break the mirror symmetry of the enantiomers by using circularly polarized light.

About 20 years ago, cyclic three-level systems of chiral molecules [13,14] were proposed with applying three electromagnetic fields (optical or microwave fields) to couple with the three electronic-dipole transitions, respectively. Such cyclic three-level systems of chiral molecules are similar for both left- and right-handed chiral molecules with only a sign difference in one of the Rabi frequencies (coupling strengths). Based on the cyclic three-level systems, the enantiomer-specific state transfer (ESST) of chiral molecules has been achieved with an adiabatical passage [13]. For the left- and right-handed chiral molecules in the initial ground states, they will evolve finally to different-energy states. After the achievement of ESST, one can further realize the spatial enantioseparation by a variety of energy-dependent processes [15] or the enantiodiscrimination for the chiral molecules. In the previous works of enantiodiscrimination [9–12], the magnetic-dipole or electrical-quadrupole interactions (which are weak usually) are involved and thus the chiral signal is weak. In contrast, the ESST based on cyclic three-level systems, where only the electric-dipole interactions are involved, provides an alternative method for enantiodiscrimination. Moreover, based on the similar cyclic three-level (sub-)systems, the direct enantiodiscrimination [16–27] and spatial enantioseparation [15,28–31] (together with enantioconversion [14,32–35]) have also been proposed.

In the original method of ESST [13], the ESST process is slow and complicated due to the requirement of adiabatic passage (together with diabatic passage). In order to obtain the faster ESST process, a dynamic method of ESST [36,37] was proposed by using several short resonant pulses in the similar cyclic three-level systems. Experimentally, ESST of chiral molecules were demonstrated in cyclic three-level systems by applying three microwave fields dynamically [38–43]. Recently, the fast method of shortcuts to adiabaticity to achieve the ESST [44] was proposed by using dynamic short-pulse operations. Several interesting theoretical methods of ESST with other problems were also proposed and developed [45–54].

In this paper we propose a streamlined and efficient method to realize the fast ESST of chiral molecules in cyclic three-level systems. The basic strategy of our method is to inversely engineer the Hamiltonian of the cyclic three-level system to achieve desired state transfer. When the Hamiltonian of the three-level chiral molecules possesses the specific SU(2)

*yongli@hainanu.edu.cn
†zhanglincn@snnu.edu.cn

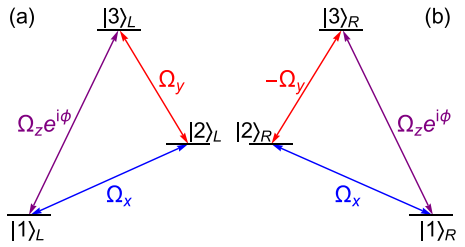

FIG. 1. (a) Left- and (b) right-handed chiral molecules of cyclic three-level systems. Three electromagnetic fields couple, respectively, to the three electric-dipole transitions with Ω_x, $\pm\Omega_y$, and $\Omega_z e^{i\phi}$ the corresponding Rabi frequencies.

algebraic structure, the populations occupying the two excited states are shown to be exchanged between the left- and right-handed chiral molecules if they are initially in their ground states. This will facilitate a streamlined physical mechanism to implement the fast ESST. Here we focus on designing a neat process of population transfer to the target excited state for only one type of enantiomers (e.g., left-handed chiral molecules). Correspondingly, the specific SU(2) algebraic structures of the system enable the right-handed chiral molecules to automatically access a population transfer to the other excited state from their ground states, simultaneously. By utilizing a SU(2) transformation [55,56], the fast ESST is achieved with choosing suitable parameters to make the left-handed (right-handed) chiral molecules ultimately evolve to one (the other one) of the excited states.

II. CYCLIC THREE-LEVEL SYSTEMS WITH SU(2) STRUCTURES

The two enantiomers can be modeled simultaneously as cyclic three-level systems (see Fig. 1) based on electric-dipole transitions [13,57]. Here we only consider the case that all the three electromagnetic fields couple resonantly to the electric-dipole transitions, respectively. Hence the Hamiltonians of the cyclic three-level systems for the two enantiomers in the basis $|m\rangle_L$ and $|m\rangle_R$ $(m = 1, 2, 3)$ can be described in the interaction picture as ($\hbar = 1$) [44]

$$\hat{H}^{L,R}(t) = \begin{pmatrix} 0 & \Omega_x(t) & \Omega_z(t)e^{-i\phi} \\ \Omega_x(t) & 0 & \pm\Omega_y(t) \\ \Omega_z(t)e^{i\phi} & \pm\Omega_y(t) & 0 \end{pmatrix}, \quad (1)$$

where the indices L and R denote, respectively, the left- and right-handed chiral molecules. Here Ω_j $(j = x, y, z)$ are the Rabi frequencies, which can be controlled by varying the amplitudes of the applied electromagnetic fields. Without loss of generality, we have assumed Ω_j are real. ϕ is the overall phase of the three Rabi frequencies. The only difference between the two enantiomers is the sign before the Rabi frequency Ω_y. As seen in Eq. (1), the $+(-)$ sign corresponds to left- (right-) handed chiral molecules. This will inspire us to realize ESST from a different perspective.

Now we consider a general cyclic three-level system with its Hamiltonian being the same form as that for the left-handed chiral molecules in Eq. (1). From now on we focus on the case

$$\Omega_x = \Omega_z \equiv \Omega, \ \phi = \pi/2. \quad (2)$$

The related Hamiltonian can be expressed in the basis of $\{|1\rangle, |2\rangle, |3\rangle\}$ as

$$\hat{H}(t) = \Omega(t)\hat{K}_x + \Omega_y(t)\hat{K}_y + \Omega(t)\hat{K}_z, \quad (3)$$

with $|1\rangle = (1, 0, 0)^T$, $|2\rangle = (0, 1, 0)^T$, $|3\rangle = (0, 0, 1)^T$. Here, $\hat{K}_x$, $\hat{K}_y$, and $\hat{K}_z$ are angular-momentum operators [58]:

$$\hat{K}_x = \begin{pmatrix} 0 & 1 & 0 \\ 1 & 0 & 0 \\ 0 & 0 & 0 \end{pmatrix}, \ \hat{K}_y = \begin{pmatrix} 0 & 0 & 0 \\ 0 & 0 & 1 \\ 0 & 1 & 0 \end{pmatrix}, \ \hat{K}_z = \begin{pmatrix} 0 & 0 & -i \\ 0 & 0 & 0 \\ i & 0 & 0 \end{pmatrix}. \quad (4)$$

They satisfy the commutation relations

$$[\hat{K}_x, \hat{K}_y] = i\hat{K}_z, \quad [\hat{K}_y, \hat{K}_z] = i\hat{K}_x, \quad [\hat{K}_z, \hat{K}_x] = i\hat{K}_y. \quad (5)$$

Note that the Hamiltonian (3) is written as a sum of three SU(2) operators. That means it addresses the SU(2) algebraic structure [59]. Based on such a structure with the condition (2), we will further investigate the ESST in following sections. Note that the condition (2) is always possible to fulfill for the single-loop cyclic three-level system of chiral molecules in experiments by appropriately adjusting the amplitudes and initial phases of the three electromagnetic fields, instead of depending on specific molecular parameters. We would also like to point out that an alternative condition $\Omega_x = \Omega_z \equiv \Omega$ and $\phi = -\pi/2$ would also work for the achievement of ESST, similar to the case of condition (2). Here we only focus on condition (2).

III. THE EXCHANGE SYMMETRY OF POPULATIONS IN THE TWO EXCITED STATES

We consider the general Hamiltonian for the cyclic three-level system with the SU(2) algebraic structure described by the Hamiltonian (3), which can be expressed in the basis of $\{|1\rangle, |2\rangle, |3\rangle\}$ as

$$\hat{H}(t) = \begin{pmatrix} 0 & \Omega & -i\Omega \\ \Omega & 0 & \Omega_y \\ i\Omega & \Omega_y & 0 \end{pmatrix}. \quad (6)$$

By introducing a new basis $\{|1'\rangle, |2'\rangle, |3'\rangle\}$ with $|1'\rangle = |1\rangle$, $|2'\rangle = i|3\rangle$, and $|3'\rangle = -i|2\rangle$, the Hamiltonian $\hat{H}(t)$ can be reexpressed as

$$\hat{H}(t) = \begin{pmatrix} 0 & \Omega & -i\Omega \\ \Omega & 0 & -\Omega_y \\ i\Omega & -\Omega_y & 0 \end{pmatrix}'. \quad (7)$$

Here the prime is used to emphasize the basis of $\{|1'\rangle, |2'\rangle, |3'\rangle\}$.

The corresponding evolution states are $|\psi(t)\rangle = C_1(t)|1\rangle + C_2(t)|2\rangle + C_3(t)|3\rangle$ for Eq. (6) and $|\psi(t)\rangle = C'_1(t)|1'\rangle + C'_2(t)|2'\rangle + C'_3(t)|3'\rangle$ for Eq. (7). Therefore we obtain

$$C_1(t) = C'_1(t), \quad C_2(t) = -iC'_3(t), \quad C_3(t) = iC'_2(t). \quad (8)$$

That is, the related populations for the energy levels, defined as $P_m(t) = |C_m(t)|^2$ and $P'_m(t) = |C'_m(t)|^2$, satisfy

$$P_1(t) = P'_1(t), \quad P_2(t) = P'_3(t), \quad P_3(t) = P'_2(t). \quad (9)$$

Note that when the Hamiltonian of the left-handed chiral molecules in the basis $\{|m\rangle_L\}$ has the same form as Eq. (6), the corresponding Hamiltonian of the right-handed chiral molecules in the basis $\{|m\rangle_R\}$ should have the same form as Eq. (7). According to Eq. (9), for the left- and right-handed chiral molecules with the similar initial states (e.g., $|1\rangle_{L,R}$), we have

$$P_1^L(t) = P_1^R(t), \quad P_2^L(t) = P_3^R(t), \quad P_3^L(t) = P_2^R(t), \tag{10}$$

which mean the populations occupying the two excited states are exchanged for the two enantiomers at all the evolution times.

IV. GENERAL TIME EVOLUTION BY THE SU(2) TRANSFORMATION

For the cyclic three-level system described by Eq. (3), the corresponding Schrödinger equation is

$$i\partial_t|\psi(t)\rangle = \hat{H}(t)|\psi(t)\rangle, \tag{11}$$

with the evolution state $|\psi(t)\rangle = \hat{U}(t)|\psi(0)\rangle$ and the evolution operator

$$\hat{U}(t) = \mathcal{T}\exp[-i\int_0^t \hat{H}(t')dt']. \tag{12}$$

In order to design the evolution path of the system, we use the unitary SU(2) transformation defined by $|\psi_S(t)\rangle = \hat{S}^\dagger(t)|\psi(t)\rangle$ with

$$\hat{S}(t) \equiv \hat{S}(\alpha,\theta,\beta) = e^{i\alpha(t)\hat{K}_z}e^{-i\theta(t)\hat{K}_y}e^{i\beta(t)\hat{K}_z}, \tag{13}$$

where α, θ, and β are time-dependent real functions (which will be further determined on demand).

After the transformation, we have the Schrödinger equation

$$i\partial_t|\psi_S(t)\rangle = \hat{H}_S(t)|\psi_S(t)\rangle \tag{14}$$

with the transformed Hamiltonian

$$\hat{H}_S(t) = \hat{S}^\dagger(t)\hat{H}(t)\hat{S}(t) + i[\partial_t\hat{S}^\dagger(t)]\hat{S}(t). \tag{15}$$

The explicit form of $\hat{H}_S(t)$ is given as

$$\hat{H}_S(t) = f_x(t)\hat{K}_x + f_y(t)\hat{K}_y + f_z(t)\hat{K}_z, \tag{16}$$

with the time-dependent coefficients

$$\begin{aligned} f_x :=& \Omega\cos\alpha\cos\beta\cos\theta - \Omega\sin\alpha\sin\beta \\ &-\Omega_y\sin\alpha\cos\beta\cos\theta - \Omega_y\cos\alpha\sin\beta \\ &-\Omega\cos\beta\sin\theta + \dot{\theta}\sin\beta - \dot{\alpha}\cos\beta\sin\theta, \\ f_y :=& \Omega\cos\alpha\sin\beta\cos\theta + \Omega\sin\alpha\cos\beta \\ &-\Omega_y\sin\alpha\sin\beta\cos\theta + \Omega_y\cos\alpha\cos\beta \\ &-\Omega\sin\beta\sin\theta - \dot{\theta}\cos\beta - \dot{\alpha}\sin\beta\sin\theta, \\ f_z :=& \Omega\cos\alpha\sin\theta - \Omega_y\sin\alpha\sin\theta + \Omega\cos\theta \\ &+\dot{\beta} + \dot{\alpha}\cos\theta. \end{aligned} \tag{17}$$

And the corresponding time-evolution operator is

$$\hat{U}_S(t) = \mathcal{T}\exp\left[-i\int_0^t \hat{H}_S(t')dt'\right]. \tag{18}$$

In order to remove the time-ordering operator $\mathcal{T}$ of $\hat{U}_S(t)$, we can properly choose the parameters (i.e., α, θ, and β) to design $\hat{H}_S(t)$ as the form $\hat{H}_S(t) = f_j(t)\hat{K}_j$ ($j = x, y, z$). In this case, the time-evolution operator reduces to

$$\hat{U}_S(t) = e^{-i\int_0^t \hat{H}_S(t')dt'} = e^{-i\delta_j(t)\hat{K}_j}, \tag{19}$$

where $\delta_j(t) = \int_0^t f_j(t')dt'$. Correspondingly, before the SU(2) transformation, the time-evolution operator

$$\hat{U}(t) = \hat{S}(t)\hat{U}_S(t)\hat{S}^\dagger(0) \tag{20}$$

can be expressed as [60]

$$\hat{U}(t) = \sum_{n=1}^{3}|\phi_n(t)\rangle\langle\phi_n(0)|, \tag{21}$$

where $\{|\phi_n(t)\rangle\}$ are a set of orthogonal time-dependent states (their explicit forms depend on the detailed form of $\hat{H}_S(t)$ and will be given below for the specific case under consideration). According to Eq. (21), for an initial state $|\phi_n(0)\rangle$, it will evolve to $|\phi_n(t)\rangle$ at any time t. This enables a dynamical passage with no transitions among the three time-dependent states during the time evolution.

By setting $\hat{H}_S(t)$ equal to one of $f_j(t)\hat{K}_j$ ($j = x, y, z$), we can obtain the explicit forms of $\Omega(t)$ and $\Omega_y(t)$. Here we choose the case of $\hat{H}_S(t) = f_z(t)\hat{K}_z$, which implies that the coefficients of $\hat{K}_x$ and $\hat{K}_y$ in Eq. (16) are zero: $f_x(t) = 0$ and $f_y(t) = 0$. For simplicity, hereafter we take $\beta = 0$ to illustrate the specific design process. Then we can obtain the Rabi frequencies

$$\begin{aligned} \Omega &= \frac{\dot{\alpha}\cos\alpha\sin\theta + \dot{\theta}\cos\theta\sin\alpha}{\cos\theta - \cos\alpha\sin\theta}, \\ \Omega_y &= -\frac{\dot{\alpha}\sin\alpha\sin\theta - \dot{\theta}(\cos\alpha\cos\theta - \sin\theta)}{\cos\theta - \cos\alpha\sin\theta}, \end{aligned} \tag{22}$$

and the time-evolution operator after the transformation reads

$$\hat{U}_S(t) = e^{-i\delta_z(t)\hat{K}_z}, \tag{23}$$

where $\delta_z(t) = \int_0^t f_z(t')dt'$ is given as

$$\delta_z(t) = \int_0^t \frac{\dot{\alpha}(t') + \dot{\theta}(t')\sin\alpha(t')}{\cos\theta(t') - \cos\alpha(t')\sin\theta(t')}dt'. \tag{24}$$

Therefore, the time-evolution operator before the SU(2) transformation is

$$\hat{U}(t) = e^{i\alpha(t)\hat{K}_z}e^{-i\theta(t)\hat{K}_y}e^{i\delta_z(t)\hat{K}_z}e^{i\theta(0)\hat{K}_y}e^{-i\alpha(0)\hat{K}_z}. \tag{25}$$

Combined with Eq. (21), the corresponding orthogonal time-dependent states are obtained as

$$\begin{aligned} |\phi_1(t)\rangle &= \begin{pmatrix} \cos\alpha(t)\cos\delta_z(t) - \sin\alpha(t)\cos\theta(t)\sin\delta_z(t) \\ i\sin\theta(t)\sin\delta_z(t) \\ -\sin\alpha(t)\cos\delta_z(t) - \cos\alpha(t)\cos\theta(t)\sin\delta_z(t) \end{pmatrix}, \\ |\phi_2(t)\rangle &= \begin{pmatrix} -i\sin\alpha(t)\sin\theta(t) \\ \cos\theta(t) \\ -i\cos\alpha(t)\sin\theta(t) \end{pmatrix}, \\ |\phi_3(t)\rangle &= \begin{pmatrix} \sin\alpha(t)\cos\theta(t)\cos\delta_z(t) + \cos\alpha(t)\sin\delta_z(t) \\ -i\sin\theta(t)\cos\delta_z(t) \\ \cos\alpha(t)\cos\theta(t)\cos\delta_z(t) - \sin\alpha(t)\sin\delta_z(t) \end{pmatrix}. \end{aligned} \tag{26}$$

V. INVERSELY ENGINEERING THE HAMILTONIAN TO ACHIEVE ENANTIOMER-SPECIFIC STATE TRANSFER

We now specify an inversely engineered $\hat{H}(t)$ for the general cyclic three-level system to achieve the desired population transfer. Suppose we aim to obtain the population transfer from the initial state $|1\rangle$ to the final target one $|2\rangle$. Then the time-evolution operator in Eq. (25) with the orthogonal time-dependent states in Eq. (26) can guarantee such a fast population transfer passage if we take $|\phi_2(0)\rangle = -i(1,0,0)^T = -i|1\rangle$ as the initial state and $|\phi_2(\tau)\rangle = (0,1,0)^T = |2\rangle$ as the target state at a given final time τ. Note that here a global phase $3\pi/2$ appears before $|1\rangle$ for the initial state. In fact, such a global phase for the initial state does not matter here and would not bring any effects to the excitation process (e.g., under the same operation, if we take $|\phi_2(0)\rangle = (1,0,0)^T = |1\rangle$ as the initial state, then we will obtain the target state $|\phi_2(\tau)\rangle = i(0,1,0)^T = i|2\rangle$). Using these boundary conditions, we can purposely design the time functions of the parameters $\alpha(t)$ and $\theta(t)$ to inversely engineer the Rabi functions Ω and Ω_y through Eq. (22). As there are many sets of interpolation functions that are consistent with the boundary conditions of the initial and final time instants, now we are ready to apply two different protocols of inverse engineering.

Protocol 1. In the first protocol, based on the requirements of $|\phi_2(0)\rangle = -i(1,0,0)^T = -i|1\rangle$ at the initial time and $|\phi_2(\tau)\rangle = (0,1,0)^T = |2\rangle$ at the final time τ, the boundary conditions can be given as

$$\alpha(0) = \frac{\pi}{2}, \quad \theta(0) = \frac{\pi}{2}, \quad \theta(\tau) = 0. \tag{27}$$

With these boundary conditions, one can insert a polynomial for $\alpha(t)$ and $\theta(t)$ to determine Ω and Ω_y. Here we can simply choose

$$\alpha(t) = \frac{\pi}{2}, \quad \theta(t) = \frac{\pi}{2}\left(1 - \frac{t}{\tau}\right). \tag{28}$$

Thus the designed Rabi frequencies in Eq. (22) reduce to

$$\Omega = \dot{\theta}, \quad \Omega_y = -\dot{\theta}\frac{\sin\theta}{\cos(\theta - \epsilon)}, \tag{29}$$

where the small value ϵ is set to avoid the infinite values of Ω_y at the initial time instant.

So far, we have shown how to achieve the population transfer of the general cyclic three-level system from the initial state $-i|1\rangle$ to the final one $|2\rangle$, following the designed Rabi frequencies in Eq. (29). For the left-handed chiral molecule whose Hamiltonian $\hat{H}^L(t)$ in Eq. (1) has the same form as the general one $\hat{H}(t)$ (3), it can also be transferred from the initial state $-i|1\rangle_L$ to the final one $|2\rangle_L$ following the designed Rabi frequencies in Eq. (29).

Figure 2(a) shows the corresponding designed Rabi frequencies for the left-handed chiral molecule in protocol 1. By following the designed Rabi frequencies in Eq. (29), the populations in the initial state $-i|1\rangle_L$ with $P_1^L(0) = 1$ are approximately transferred to that in the state $|2\rangle_L$ with $P_2^L(\tau) = 0.9946$ with a small value $\epsilon = 0.04$, as shown in Fig. 2(b). Note that in Fig. 2, the time (the Rabi frequencies) is given in the unit of τ $(2\pi/\tau)$, and the evolved populations are independent of the parameter τ.

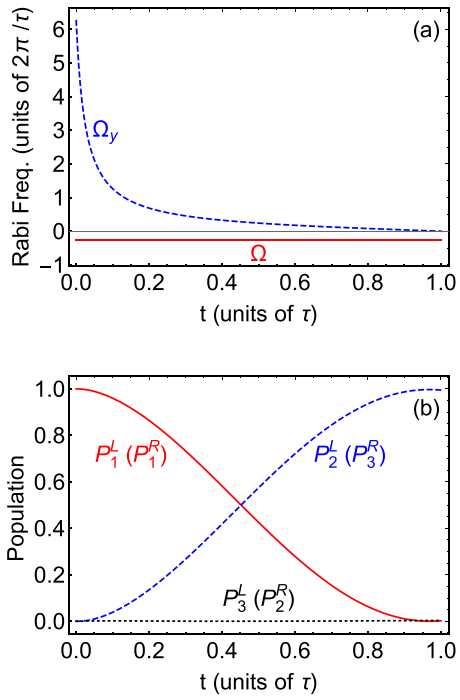

FIG. 2. (a) The designed Rabi frequencies Ω (red solid line) and Ω_y (blue dashed line) in Eq. (29) with the conditions in Eq. (28). (b) The corresponding time evolution of the populations for the left- and right-handed chiral molecules: $P_1^L(t) = P_1^R(t)$ (red solid line), $P_2^L(t) = P_3^R(t)$ (blue dashed line), and $P_3^L(t) = P_2^R(t)$ (black dotted line). Here $\epsilon = 0.04$. The initial states are $-i|1\rangle_{L,R}$.

On the other hand, the right-handed chiral molecule, whose Hamiltonian is similar to that of the left-handed one with only changing the sign before Ω_y, will evolve simultaneously following the same Rabi frequencies designed in Eq. (29). According to Eq. (10), when the left- and right-handed chiral molecules address the specific SU(2) algebraic structure, that is, their Hamiltonians have the similar forms as Eq. (3), their populations occupying the ground states are equal and their populations occupying the two excited states are exchanged at all the evolution times (assuming the initial states be the ground ones $|1\rangle_{L,R}$). As also shown in Fig. 2(b), the populations in the initial state $-i|1\rangle_R$ with $P_1^R(0) = 1$ are finally transferred approximately to that in the state $i|3\rangle_R$ with $P_3^R(\tau) = 0.9946$ for the right-handed chiral molecules, following the designed Rabi frequencies in Eq. (29). Therefore, for the same designed Rabi frequencies in Fig. 2(a), the left- and right-handed chiral molecules staying initially in the ground states $-i|1\rangle_{L,R}$ can evolve in a short time to the final states $|2\rangle_L$ and $i|3\rangle_R$, respectively, with high efficiencies. That means the fast ESST is achieved.

For the designed Rabi frequencies in protocol 1, Ω corresponds to a square pulse and Ω_y to a time-varying pulse with large intensity. Using the square pulse means the abrupt switching of the pulses, which would be harmful to the efficiency of the ESST. At the same time, we do not expect to use a pulse with too large intensity. Thus it is better to choose suitable Rabi frequencies so that both the pulses can be turned on and off smoothly (e.g., the pulses vanish smoothly at $t = 0$

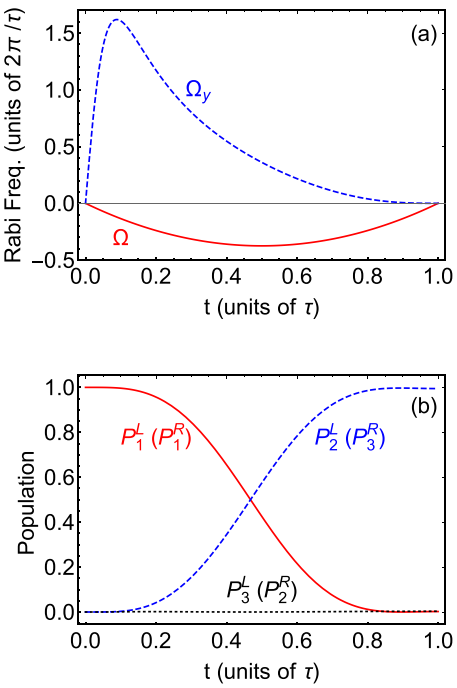

FIG. 3. (a) The designed Rabi frequencies Ω (red solid line) and Ω_y (blue dashed line) in Eq. (32) with the conditions (31). (b) The corresponding time evolution of the populations for the left- and right-handed chiral molecules: $P_1^L(t) = P_1^R(t)$ (red solid line), $P_2^L(t) = P_3^R(t)$ (blue dashed line), and $P_3^L(t) = P_2^R(t)$ (black dotted line). Here $\epsilon' = 0.04$. The initial states are $-i|1\rangle_{L,R}$.

and $t = \tau$), and the intensities of pulses can be restricted to be in a smaller range, as shown in the following protocol 2.

Protocol 2. First we still consider the general cyclic three-level system and aim to obtain the evolution from the initial state $|\phi_2(0)\rangle = -i(1, 0, 0)^T = -i|1\rangle$ to the final one $|\phi_2(\tau)\rangle = (0, 1, 0)^T = |2\rangle$. In protocol 2, we expect both the pulses (also the Rabi frequencies) vanish smoothly at $t = 0$ and $t = \tau$. Now the boundary conditions can be given as

$$\alpha(0) = \frac{\pi}{2}, \quad \theta(0) = \frac{\pi}{2}, \quad \theta(\tau) = 0,$$
$$\dot{\theta}(0) = 0, \quad \dot{\theta}(\tau) = 0. \tag{30}$$

Consistent with these boundary conditions, here we can choose

$$\alpha(t) = \frac{\pi}{2}, \quad \theta(t) = \frac{\pi}{2} - \frac{3\pi}{2\tau^2}t^2 + \frac{\pi}{\tau^3}t^3. \tag{31}$$

Following Eq. (31), one can obtain the designed Rabi frequencies,

$$\Omega = \dot{\theta}, \quad \Omega_y = -\dot{\theta}\frac{\sin\theta}{\cos(\theta - \epsilon')}, \tag{32}$$

where the small value ϵ' is set to avoid the infinite values of Ω_y at the initial time instant. Note that the Rabi frequencies designed in Eq. (32) have the similar form as those in Eq. (29). But the explicit forms of $\theta(t)$ in Eqs. (29) and (32) are different [see, respectively, Eqs. (28) and (31)].

Figure 3 shows the designed Rabi frequencies and population transfers for the left- and right-handed chiral molecules in protocol 2. The corresponding populations in the initial state $-i|1\rangle_L$ ($-i|1\rangle_R$) with $P_1^L(0) = 1$ [$P_1^R(0) = 1$] are approximately transferred to those of the final state $|2\rangle_L$ ($-i|3\rangle_R$) with $P_2^L(\tau) = 0.9946$ [$P_3^R(\tau) = 0.9946$] of the left- (right-) handed chiral molecules with the small value $\epsilon' = 0.04$.

Compared with the case of protocol 1, there exist two advantages in protocol 2: (1) Both the Rabi frequencies $\Omega(t)$ and $\Omega_y(t)$ vanish in the initial and final time instants, which avoids abrupt switching of the pulses. (2) The maximum value for the designed Rabi frequencies in protocol 2 is smaller than that in protocol 1 for the same evolution time and equal small values $\epsilon = \epsilon'$, which makes it easier to apply in experiments. Note that except for the above two protocols, there are a variety of alternative protocols to realize the similar fast ESST of chiral molecules by choosing different parameters (e.g., α and θ).

Note that in our fast dynamical method of ESST, all three optical fields are applied simultaneously. This is different from the previous fast dynamical method of ESST in Refs. [36,42], where the optical pules are applied successively. We would also like to point out that in the previous methods of ESST [13,14,36,42,44], the specific optical pulses should be designed to accomplish the complete population transfer from the ground state to a particular final state (e.g., $|1\rangle_L \to |2\rangle_L$) for the left-handed molecule and at the same time accomplish the population transfer from the ground state to the different-energy final state for the right-handed molecule (e.g., $|1\rangle_R \to |3\rangle_R$). By contrast, in our work we focus on the case that the cyclic three-level systems of two enantiomers possess the specific SU(2) algebraic structures, which guarantees the populations occupying the two excited states are exchanged for the two enantiomers if they are initially prepared in their ground states. Therefore we only need to design a simple process for the optical fields aiming at obtaining the population transfer, e.g., from states $|1\rangle_L$ to $|2\rangle_L$ for left-handed chiral molecules, since such a process would make the right-handed chiral molecules obtain automatically the population transfer from states $|1\rangle_R$ to $|3\rangle_R$ simultaneously. In a nutshell, the complete population transfer of one enantiomer guarantees a successful population transfer of the other one in this case, leading to an efficient ESST.

We would like to point out that in protocol 2, the final populations of the target states are determined by the small value ϵ' and are independent of the parameter τ, similar to the case in protocol 1. As shown in Fig. 4, the final populations can be further improved by decreasing the small value ϵ' [see Fig. 4(b)], but decreasing the small amount ϵ' implies the tradeoff of requiring larger Rabi frequencies and laser intensities [47,59] [see Fig. 4(a)]. Here the maximum absolute value of the Rabi frequencies during the whole evolution process is defined as $\Omega_{\max} = \text{Max}\{|\Omega|, |\Omega_y|\}$.

In experiments, the Rabi frequencies can be controlled by varying the amplitudes of the applied electromagnetic fields. Typical experimentally available Rabi frequencies for the transitions of chiral molecules are about $2\pi \times 10$ MHz or less [18,38–40]. Hence we can choose the small value ϵ' in the region (0.005, 0.05) so that the final populations in the target states are larger than 0.990 with the maximum value of the designed Rabi frequencies being less than $2\pi \times 10$ MHz in protocol 2. This means our designed Rabi frequencies would be applicable in current experiments of chiral molecules. On

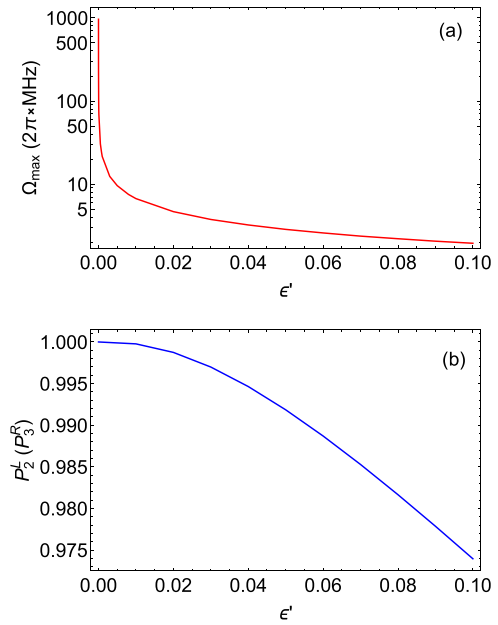

FIG. 4. (a) The maximum absolute value of the Rabi frequencies Ω_{max} vs the small value ϵ' in protocol 2 with $\tau = 0.5\,\mu s$. (b) The corresponding populations of the target states at the final time vs the small value ϵ'. The initial states are $-i|1\rangle_{L,R}$.

the other hand, in general, decoherence is one of the main obstacles in quantum-state-transfer operations. In our method, the evolution time can be shortened to 0.5 μs for the experimentally available Rabi frequencies $2\pi \times 10$ MHz. That means the effect of the decoherence (typically about $5 \sim 6\,\mu s$ [17,38]) is negligible in our method involving a fast dynamical process. In addition, we have assumed the Rabi frequencies (and equivalently, the amplitudes of the electromagnetic fields) are uniform for all the molecules. This requires the characteristic length of the molecular sample in experiments should be much smaller than the beam radii of the electromagnetic fields (typically of the order of the wavelengths of the electromagnetic fields) so that the Rabi frequencies are approximately the same for all the molecules.

VI. CONCLUSION

In conclusion, we have proposed a streamlined method to realize the fast ESST of chiral molecules based on the cyclic three-level systems. When the Hamiltonians of the three-level chiral molecules possess the specific SU(2) algebraic structures, the populations occupying the two excited states are exchanged between the left- and right-handed chiral molecules at all the evolution times if prepared initially in their corresponding ground states. This means that the ESST can be achieved by focusing on designing the desired population transfer for only one enantiomer, instead of designing simultaneously the processes of desired population transfer for the two enantiomers, respectively. By means of the unitary SU(2) transformation with large freedoms to design the appropriate parameters, the related time-evolution operator (as well as the evolved state) can be determined in a simple way without involving the time-ordering calculation. Moreover, by inversely engineering the Rabi frequencies, two protocols are shown to make the two enantiomers ultimately evolve to different excited states to achieve the fast ESST. After the achievement of the fast ESST, it allows further spatial separation of the chiral molecules with different chiralities or discrimination of their chiralities.

We would like to point out that our ESST method is performed in a nonadiabatic process and is thus faster than the previous slow adiabatic processes [13,14]. Unlike the case of nonadiabatic dynamic methods of ESST [36,42,49,52] with sequential optical pulses, here we have applied all the three electromagnetic fields simultaneously to realize fast ESST. Therefore our method may be faster than these previous nonadiabatic dynamic methods due to fewer operation steps and operation times. Moreover, in the fast shortcuts-to-adiabaticity method of ESST [44] and nonadiabatic dynamic method of ESST [46], three electromagnetic fields are also applied simultaneously. But the desired population transfer processes for both enantiomers should be designed in Refs. [44,46]. By contrast, our method focuses on only designing a neat process of population transfer for one enantiomer with the specific SU(2) algebraic structure of the system, enabling the other enantiomer to automatically access a desired population transfer simultaneously to achieve the fast ESST, which dramatically simplifies the control procedure. Therefore our method of fast ESST has promising applications in discriminating molecular chirality and controlling the dynamics of chiral molecules.

ACKNOWLEDGMENT

This work was supported by the Natural Science Foundation of China (Grants No. 12074030, No. 12274107, No. U1930402, No. 11447025, and No. 11847308).

[1] R. G. Woolley, Quantum theory and molecular structure, Adv. Phys. **25**, 27 (1976).

[2] K. T. Barrett, A. J. Metrano, P. R. Rablen, and S. J. Miller, Spontaneous transfer of chirality in an atropisomerically enriched two-axis system, Nature (London) **509**, 71 (2014).

[3] T. J. Leitereg, D. G. Guadagni, J. Harris, T. R. Mon, and R. Teranishi, Sensory evaluation spectrum method as a descriptive sensory analysis, J. Agric. Food Chem. **19**, 785 (1971).

[4] A. R. Ribeiro, P. M. L. Castro, and M. E. Tiritan, Environmental fate of chiral pharmaceuticals: Determination, degradation and toxicity, Environ. Chem. Lett. **10**, 239 (2012).

[5] R. McKendry, M. E. Theoclitou, T. Rayment, and C. Abell, Chiral discrimination by chemical force microscopy, Nature (London) **391**, 566 (1998).

[6] G. L. J. A. Rikken and E. Raupach, Chirality, magnetism and light, Nature (London) **405**, 932 (2000).

[7] *Chiral Separation Methods for Pharmaceutical and Biotechnological Products*, edited by S. Ahuja (John Wiley & Sons, New York, 2011).

[8] H. Zepik, E. Shavit, M. Tang, T. R. Jensen, K. Kjaer, G. Bolbach, L. Leiserowitz, I. Weissbuch, and M. Lahav, Chiral amplification of oligopeptides in two-dimensional crystalline self-assemblies on water, Science **295**, 1266 (2002).

[9] N. Berova and K. Nakanishi, *Circular Dichroism: Principles and Applications* (Wiley, New York, 2000).

[10] L. A. Nafie, T. A. Keiderling, and P. J. Stephens, Vibrational circular dichroism, J. Am. Chem. Soc. **98**, 2715 (1976).

[11] R. Kondru, P. Wipf, and D. Beratan, Atomic contributions to the optical rotation angle as a quantitative probe of molecular chirality, Science **282**, 2247 (1998).

[12] L. D. Barron, F. Zhu, L. Hecht, G. E. Tranter, and N. W. Isaacs, Raman optical activity: An incisive probe of molecular chirality and biomolecular structure, J. Mol. Struct. **834**, 7 (2007).

[13] P. Král and M. Shapiro, Cyclic Population Transfer in Quantum Systems with Broken Symmetry, Phys. Rev. Lett. **87**, 183002 (2001).

[14] P. Král, I. Thanopulos, M. Shapiro, and D. Cohen, Two-Step Enantio-Selective Optical Switch, Phys. Rev. Lett. **90**, 033001 (2003).

[15] Y. Li, C. Bruder, and C. P. Sun, Generalized Stern-Gerlach Effect for Chiral Molecules, Phys. Rev. Lett. **99**, 130403 (2007).

[16] W. Z. Jia and L. F. Wei, Probing molecular chirality by coherent optical absorption spectra, Phys. Rev. A **84**, 053849 (2011).

[17] D. Patterson, M. Schnell, and J. M. Doyle, Enantiomer-specific detection of chiral molecules via microwave spectroscopy, Nature (London) **497**, 475 (2013).

[18] D. Patterson and J. M. Doyle, Sensitive Chiral Analysis via Microwave Three-Wave Mixing, Phys. Rev. Lett. **111**, 023008 (2013).

[19] V. A. Shubert, D. Schmitz, D. Patterson, J. M. Doyle, and M. Schnell, Identifying enantiomers in mixtures of chiral molecules with broadband microwave spectroscopy, Angew. Chem. Int. Ed. **53**, 1152 (2014).

[20] S. Lobsiger, C. Pérez, L. Evangelisti, K. K. Lehmann, and B. H. Pate, Molecular structure and chirality detection by Fourier transform microwave spectroscopy, J. Phys. Chem. Lett. **6**, 196 (2015).

[21] V. A. Shubert, D. Schmitz, C. Pérez, C. Medcraft, A. Krin, S. R. Domingos, D. Patterson, and M. Schnell, Chiral analysis using broadband rotational spectroscopy, J. Phys. Chem. Lett. **7**, 341 (2016).

[22] C. Ye, Q. Zhang, Y. Y. Chen, and Y. Li, Determination of enantiomeric excess with chirality-dependent ac Stark effects in cyclic three-level models, Phys. Rev. A **100**, 033411 (2019).

[23] C. Ye, Y. Sun, and X. Zhang, Entanglement-assisted quantum chiral spectroscopy, J. Phys. Chem. Lett. **12**, 8591 (2021).

[24] M. R. Cai, C. Ye, H. Dong, and Y. Li, Enantiodetection of Chiral Molecules via Two-Dimensional Spectroscopy, Phys. Rev. Lett. **129**, 103201 (2022).

[25] Y. Y. Chen, C. Ye, and Y. Li, Enantio-detection via cavity-assisted three-photon processes, Opt. Express **29**, 36132 (2021).

[26] Y. Y. Chen, J. J. Cheng, C. Ye, and Y. Li, Enantiodetection of cyclic three-level chiral molecules in a driven cavity, Phys. Rev. Res. **4**, 013100 (2022).

[27] F. Zou, Y. Y. Chen, B. Liu, and Y. Li, Enantiodiscrimination of chiral molecules via quantum correlation function, Opt. Express **30**, 31073 (2022).

[28] X. Li and M. Shapiro, Theory of the optical spatial separation of racemic mixtures of chiral molecules, J. Chem. Phys. **132**, 194315 (2010).

[29] A. Jacob and K. Hornberger, Effect of molecular rotation on enantioseparation, J. Chem. Phys. **137**, 044313 (2012).

[30] N. Kravets, A. Aleksanyan, and E. Brasselet, Chiral Optical Stern-Gerlach Newtonian Experiment, Phys. Rev. Lett. **122**, 024301 (2019).

[31] B. Liu, C. Ye, C. P. Sun, and Y. Li, Spatial enantioseparation of gaseous chiral molecules, Phys. Rev. A **104**, 013113 (2021).

[32] M. Shapiro, E. Frishman, and P. Brumer, Coherently Controlled Asymmetric Synthesis with Achiral Light, Phys. Rev. Lett. **84**, 1669 (2000).

[33] P. Brumer, E. Frishman, and M. Shapiro, Principles of electric-dipole-allowed optical control of molecular chirality, Phys. Rev. A **65**, 015401 (2001).

[34] C. Ye, Q. Zhang, Y. Y. Chen, and Y. Li, Fast enantioconversion of chiral mixtures based on a four-level double-Δ model, Phys. Rev. Res. **2**, 033064 (2020).

[35] C. Ye, B. Liu, Y. Y. Chen, and Y. Li, Enantio-conversion of chiral mixtures via optical pumping, Phys. Rev. A **103**, 022830 (2021).

[36] Y. Li and C. Bruder, Dynamic method to distinguish between left- and right-handed chiral molecules, Phys. Rev. A **77**, 015403 (2008).

[37] W. Z. Jia and L. F. Wei, Distinguishing left- and right-handed molecules using two-step coherent pulses, J. Phys. B **43**, 185402 (2010).

[38] S. Eibenberger, J. Doyle, and D. Patterson, Enantiomer-Specific State Transfer of Chiral Molecules, Phys. Rev. Lett. **118**, 123002 (2017).

[39] C. Pérez, A. L. Steber, S. R. Domingos, A. Krin, D. Schmitz, and M. Schnell, Coherent enantiomer-selective population enrichment using tailored microwave fields, Angew. Chem. Int. Ed. **56**, 12512 (2017).

[40] D. Patterson and M. Schnell, New studies on molecular chirality in the gas phase: Enantiomer differentiation and determination of enantiomeric excess, Phys. Chem. Chem. Phys. **16**, 11114 (2014).

[41] K. K. Lehmann, Influence of spatial degeneracy on rotational spectroscopy: Three-wave mixing and enantiomeric state separation of chiral molecules, J. Chem. Phys. **149**, 094201 (2018).

[42] J. H. Lee, J. Bischoff, A. O. Hernandez-Castillo, B. Sartakov, G. Meijer, and S. Eibenberger-Arias, Quantitative Study of Enantiomer-Specific State Transfer, Phys. Rev. Lett. **128**, 173001 (2022).

[43] C. Pérez, A. L. Steber, S. R. Domingos, A. Krin, D. Schmitz, and M. Schnell, Coherent enantiomer-selective population enrichment using tailored microwave fields, Angew. Chem. Int. Ed. **129**, 12686 (2017).

[44] N. V. Vitanov and M. Drewsen, Highly Efficient Detection and Separation of Chiral Molecules through Shortcuts to Adiabaticity, Phys. Rev. Lett. **122**, 173202 (2019).

[45] C. Ye, Q. Zhang, Y. Y. Chen, and Y. Li, Effective two-level models for highly efficient inner-state enantioseparation based on cyclic three-level systems of chiral molecules, Phys. Rev. A **100**, 043403 (2019).

[46] M. Leibscher, T. F. Giesen, and C. P. Koch, Principles of enantio-selective excitation in three-wave mixing spectroscopy of chiral molecules, J. Chem. Phys. **151**, 014302 (2019).

[47] J. L. Wu, Y. Wang, J. Song, Y. Xia, S. L. Su, and Y. Y. Jiang, Robust and highly efficient discrimination of chiral molecules through three-mode parallel paths, Phys. Rev. A **100**, 043413 (2019).

[48] Q. Zhang, Y.-Y. Chen, C. Ye, and Y. Li, Evading thermal population influence on enantiomeric-specific state transfer based on a cyclic three-level system via ro-vibrational transitions, J. Phys. B: At. Mol. Opt. Phys. **53**, 235103 (2020).

[49] B. T. Torosov, M. Drewsen, and N. V. Vitanov, Efficient and robust chiral resolution by composite pulses, Phys. Rev. A **101**, 063401 (2020).

[50] J. L. Wu, Y. Wang, J. X. Han, C. Wang, S. L. Su, Y. Xia, Y. Y. Jiang, and J. Song, Two-Path Interference for Enantiomer-Selective State Transfer of Chiral Molecules, Phys. Rev. Appl. **13**, 044021 (2020).

[51] B. Liu, C. Ye, C. P. Sun, and Y. Li, Enantiospecific state transfer for gaseous symmetric-top chiral molecules, Phys. Rev. A **105**, 043110 (2022).

[52] B. T. Torosov, M. Drewsen, and N. V. Vitanov, Chiral resolution by composite Raman pulses, Phys. Rev. Res. **2**, 043235 (2020).

[53] M. Leibscher, E. Pozzoli, C. Pérez, M. Schnell, M. Sigalotti, U. Boscain, and C. P. Koch, Full quantum control of enantiomer-selective state transfer in chiral molecules despite degeneracy, Commun. Phys. **5**, 110 (2022).

[54] M. Leibscher, J. Kalveram, and C. P. Koch, Rational pulse design for enantiomer-selective microwave three-wave mixing, Symmetry **14**, 871 (2022).

[55] B.-H. Huang, Y.-H. Kang, Y.-H. Chen, Q.-C. Wu, J. Song, and Y. Xia, Fast quantum state engineering via universal SU(2) transformation, Phys. Rev. A **96**, 022314 (2017).

[56] J.-J. Cheng and L. Zhang, Implementing conventional and unconventional nonadiabatic geometric quantum gates via SU(2) transformations, Phys. Rev. A **103**, 032616 (2021).

[57] C. Ye, Q. Zhang, and Y. Li, Real single-loop cyclic three-level configuration of chiral molecules, Phys. Rev. A **98**, 063401 (2018).

[58] C. E. Carroll and F. T. Hioe, N-level quantum systems with SU(2) dynamic symmetry, J. Opt. Soc. Am. B **5**, 1335 (1988).

[59] X. Chen and J. G. Muga, Engineering of fast population transfer in three-level systems, Phys. Rev. A **86**, 033405 (2012).

[60] B. J. Liu, X. K. Song, Z. Y. Xue, X. Wang, and M. H. Yung, Plug-and-Play Approach to Nonadiabatic Geometric Quantum Gates, Phys. Rev. Lett. **123**, 100501 (2019).